Silole and Germole Complexes of Lanthanum and Cerium

Xiaofei Sun,[†a] Luca Münzfeld,[†a] Da Jin,[a] Adrian Hauser,[a] Peter W. Roesky*[a]

a Institute of Inorganic Chemistry, Karlsruhe Institute of Technology (KIT), Engesserstraße 15, 76131 Karlsruhe, Germany. E-mail: roesky@kit.edu

Table of Contents

I. Synthesis and characterization

I.1 General procedures

All air- and moisture-sensitive manipulations were performed under dry N_2 or Ar atmosphere either using standard Schlenk techniques or in an argon-filled MBraun glovebox. Et_2O, *n*-pentane, and toluene were dried using an MBraun solvent purification system (SPS-800) and degassed before usage. THF was distilled under nitrogen from potassium benzophenone ketyl. C_6D_6, and THF-d_8 were dried over Na-K alloy and degassed by freeze-pump-thaw cycles. Dipotassium salts of the silole and germole were prepared according to the literature procedures.[1] [Ln(η^8-COT)I(thf)$_3$)] (Ln = La, Ce) precursors were synthesized according to the literature procedures.[2] All other chemicals were obtained from commercial sources and used without further purification.

NMR spectra were recorded on Bruker spectrometers (Avance III 300 MHz, Avance 400 MHz or Avance III 400 MHz). Chemical shifts are referenced internally using signals of the residual protio solvent (^{1}H) or the solvent ($^{13}C\{^1H\}$) and are reported relative to tetramethylsilane (^{1}H, $^{13}C\{^1H\}$), or externally relative to tetramethylsilane (^{29}Si). All NMR spectra were measured at 298 K, unless otherwise specified. The multiplicity of the signals is indicated as s = singlet, d = doublet, dd = doublet of doublets, t = triplet, q = quartet, m = multiplet and br = broad. Assignments were determined based on unambiguous chemical shifts, coupling patterns and ^{13}C-DEPT experiments or 2D correlations (^{1}H-^{1}H COSY, ^{1}H-^{13}C HMQC and ^{1}H-^{13}C HMBC).

Potential Hazards: Potassium and organometallic potassium reagents may violently react with moisture, water and air, particular attention need to be paid. All products **1**-**3** are highly pyrophoric and must be handled with caution.

I.2 [K(thf)$_3$(μ-η^8:η^8-COT)La(η^5-L^{Si})]$_2$ (1)
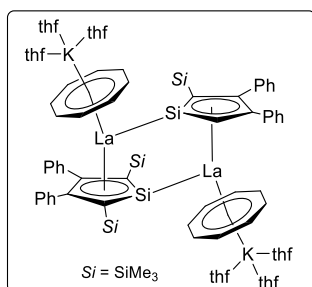
To a mixture of dichlorosilole (0.150 g, 0.335 mmol) and K (0.131 g, 3.35 mmol) was added THF (10 mL), and the resulting mixture was stirred at room temperature for 48 h. The deep brown solution was filtered to remove KCl and the excess amount of K. The THF solution of [K$_2$][L^{Si}] was added dropwise to a THF solution of [La(η^8-COT)I(thf)$_3$)] (0.196 g, 0.335 mmol) at −88 °C and the reaction mixture was stirred at −88 °C for 1 h before it was allowed to warm up to room temperature. The reaction mixture was then stirred at room temperature for 12 h and filtered. Suitable crystals for X-ray diffraction analysis were obtained by slow evaporation of the THF solution at 5 °C.

Yield (based on crystals): 0.059 g, 25%.

Due to the pyrophoric nature of **1**, no meaningful elemental analysis and IR spectrum could be obtained. Immediate thermal decomposition was observed during Raman spectroscopic analysis.

^{1}H NMR (400.30 MHz, THF-d_8): δ (ppm) = 6.96 (tm, $^3J_{HH}$ ≈ 7.1 Hz, 8H, CH_{Ph}), 6.87 (tm, $^3J_{HH}$ ≈ 7.2 Hz, 4H, CH_{Ph}), 6.78-6.76 (m, 8H, CH_{Ph}), 6.22 (s, 16H, CH_{COT}), 3.64-3.60 (m, α-C$H_{2\,thf}$), 1.79-1.76 (m, β-C$H_{2\,thf}$), −0.02 (s, 36H, Si(CH_3)$_3$).

^{13}C{^{1}H} NMR (100.67 MHz, THF-d_8): δ (ppm) = 156.9 ($C_{\alpha\,LSi}$), 150.2 ($C_{\beta\,LSi}$), 147.3 ($C_{q\,Ph}$), 130.3 (C_{Ph}), 127.4 (C_{Ph}), 124.6 (C_{Ph}), 96.9 (C_{COT}), 68.4 ($C_{\beta\,thf}$), 26.6 ($C_{\alpha\,thf}$), 5.3 (Si(CH_3)$_3$).

^{29}Si{^{1}H} NMR (79.52 MHz, THF-d_8): δ (ppm) = 187.9 (SiC$_4$), −13.9 (SiMe$_3$).

I.3 [{K(thf)(μ-η^8:η^8-COT)La(η^5-L^{Ge})}$_2$]$_n$ (2)
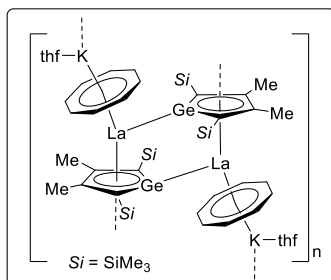
To a mixture of dichlorogermole (0.120 g, 0.326 mmol) and K (0.125 g, 3.20 mmol) was added THF (10 mL), and the resulting mixture was stirred at room temperature for 48 h. The deep brown solution was filtered to remove KCl and the excess amount of K. The THF solution of [K$_2$][L^{Ge}] was added dropwise to a THF solution of [La(η^8-COT)I(thf)$_3$)] (0.191 g, 0.326 mmol) at −88 °C and the reaction mixture was stirred at −88 °C for 1 h before it was allowed to warm up to room temperature. The reaction mixture was then stirred at room temperature for 12 h and filtered. Suitable crystals for X-ray diffraction analysis were obtained by slow evaporation of the THF solution at room temperature.

Yield (based on crystals): 0.069 g (34%).

Due to the pyrophoric nature of **2**, no meaningful elemental analysis and IR spectrum could be obtained. Immediate thermal decomposition was observed during Raman spectroscopic analysis.

^{1}H NMR (400.30 MHz, THF-d_8/C$_6$D$_6$): δ (ppm) = 6.17 (s, 16H, CH_{COT}), 3.64-3.60 (m, α-C$H_{2\,thf}$), 2.45 (s, 12H C(CH_3)), 1.79-1.76 (m, β-C$H_{2\,thf}$), 0.14 (s, 36H, Si(CH_3)$_3$).

^{13}C{^{1}H} NMR (100.67 MHz, THF-d_8/C$_6$D$_6$): δ (ppm) = 162.3 ($C_{\alpha\,LGe}$), 144.3 ($C_{\beta\,LGe}$), 96.4 (C_{COT}), 68.4 ($C_{\beta\,thf}$), 26.6 ($C_{\alpha\,thf}$), 5.5 (Si(CH_3)$_3$).

^{29}Si{^{1}H} NMR (79.52 MHz, THF-d_8/C$_6$D$_6$): δ (ppm) = −16.4.

I.4 [{K$_{0.5}$(μ-η^8:η^8-COT)Ce(η^5-L^{Ge})K(thf)(μ-η^8:η^8-COT)Ce(μ-η^8:η^8-COT)K$_{0.5}$(thf)$_{0.5}$}$_2$]$_n$ (3)
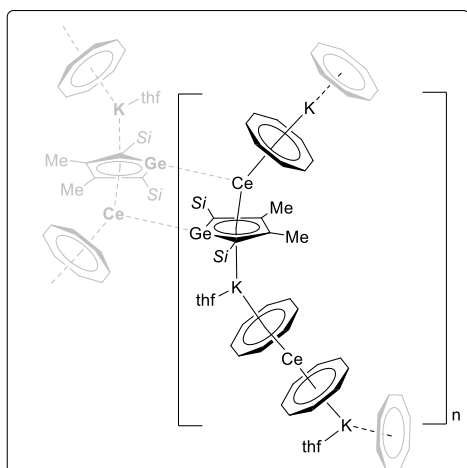
To a mixture of dichlorogermole (0.120 g, 0.326 mmol) and K (0.125 g, 3.20 mmol) was added THF (10 mL), and the resulting mixture was stirred at room temperature for 48 h. The deep brown solution was filtered to remove KCl and the excess amount of K. The THF solution of [K$_2$][L^{Ge}] was added dropwise to a THF solution of [Ce(η^8-COT)I(thf)$_3$)] (0.383 g, 0.652 mmol) at −88 °C and the reaction mixture was stirred at −88 °C for 1 h before it was allowed to warm up to room temperature. The reaction mixture was then stirred at room temperature for 12 h and filtered. Suitable crystals for X-ray diffraction analysis were obtained by slow evaporation of the THF solution at room temperature.

Yield (based on crystals): 0.047 g (20%).

Due to the pyrophoric nature of **3**, no meaningful elemental analysis and IR spectrum could be obtained. Immediate thermal decomposition was observed during Raman spectroscopic analysis. The paramagnetic character of **3** prohibited the acquisition of NMR spectra.
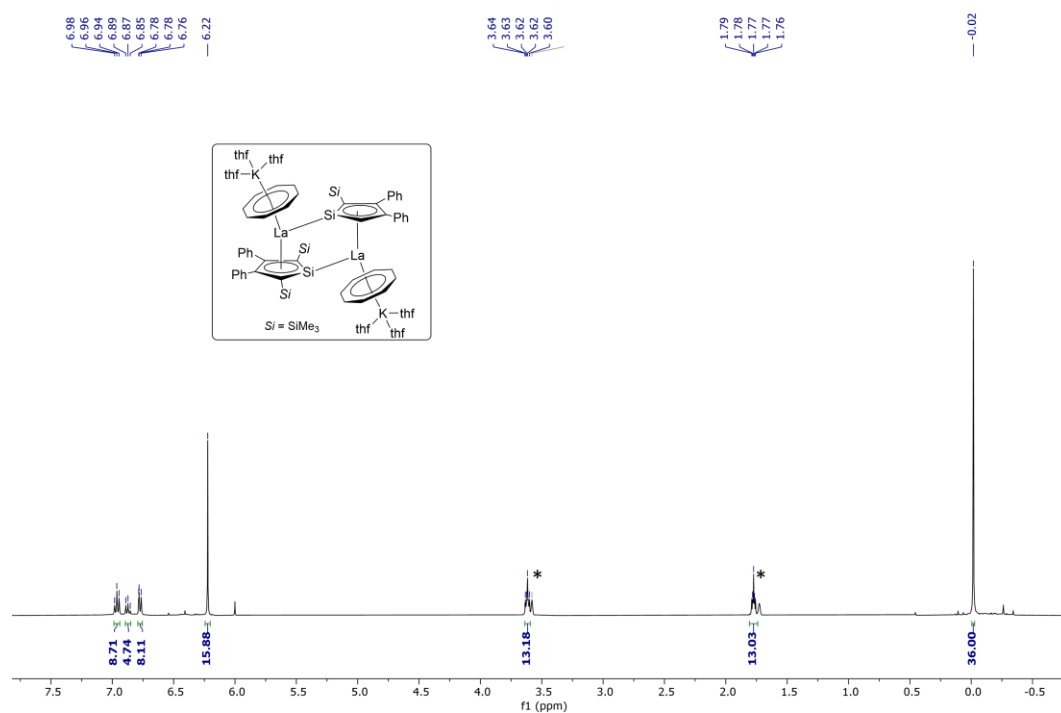
II. NMR spectra

Figure S1. ^{1}H NMR spectrum of compound **1** in THF-d_8, *, residual protio solvent signal.

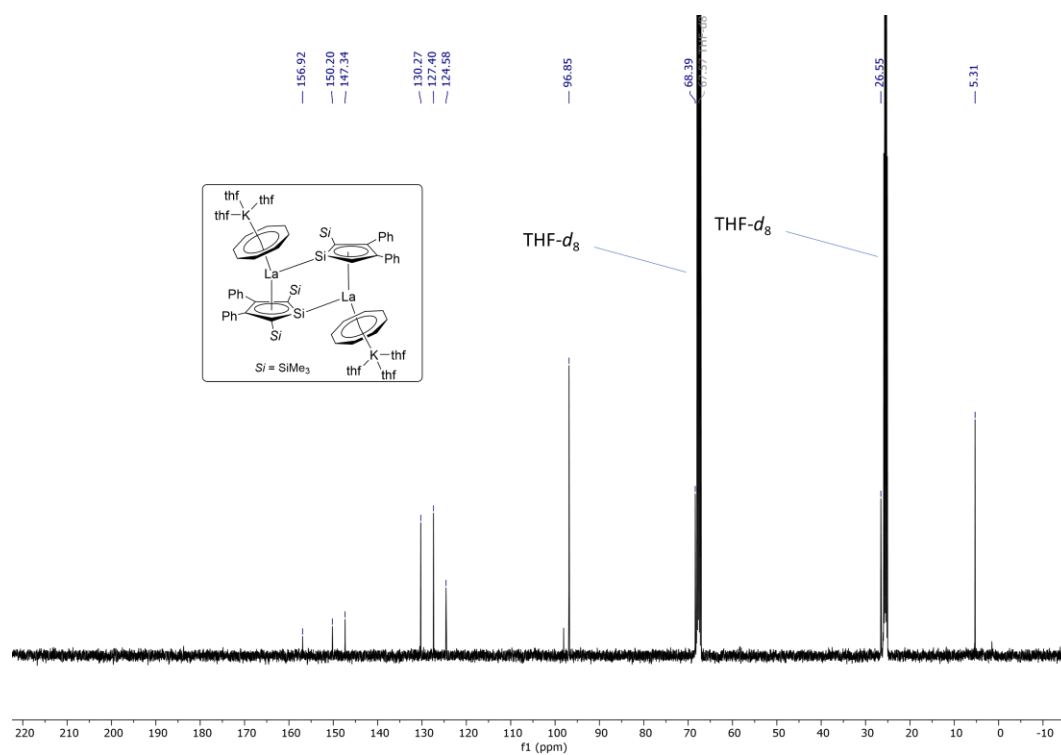**Figure S2.** ^{13}C{^{1}H} NMR spectrum of compound **1** in THF-d_8.

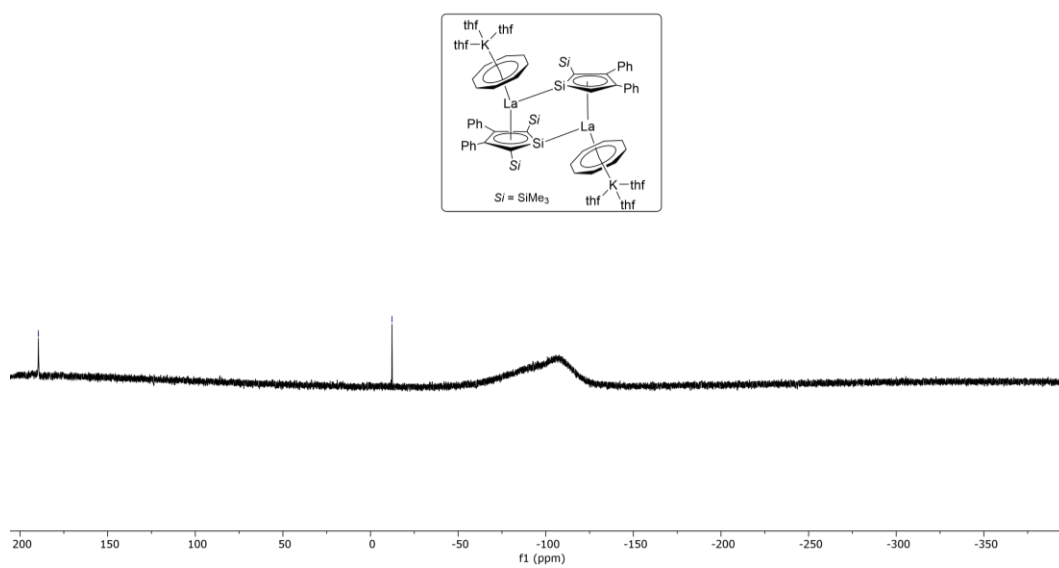**Figure S3.** $^{29}Si\{^1H\}$ NMR spectrum of compound **1** in THF-d_8.
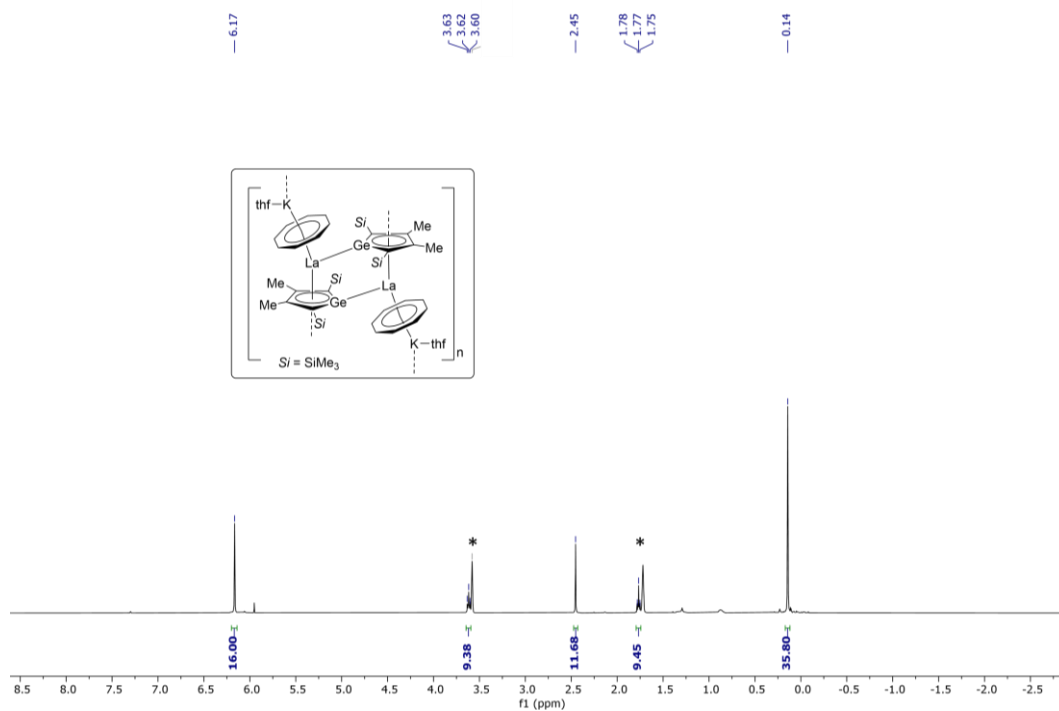
Figure S4. ^1H NMR spectrum of compound **2** in THF-d_8/C_6D_6, *, residual protio solvent signal.
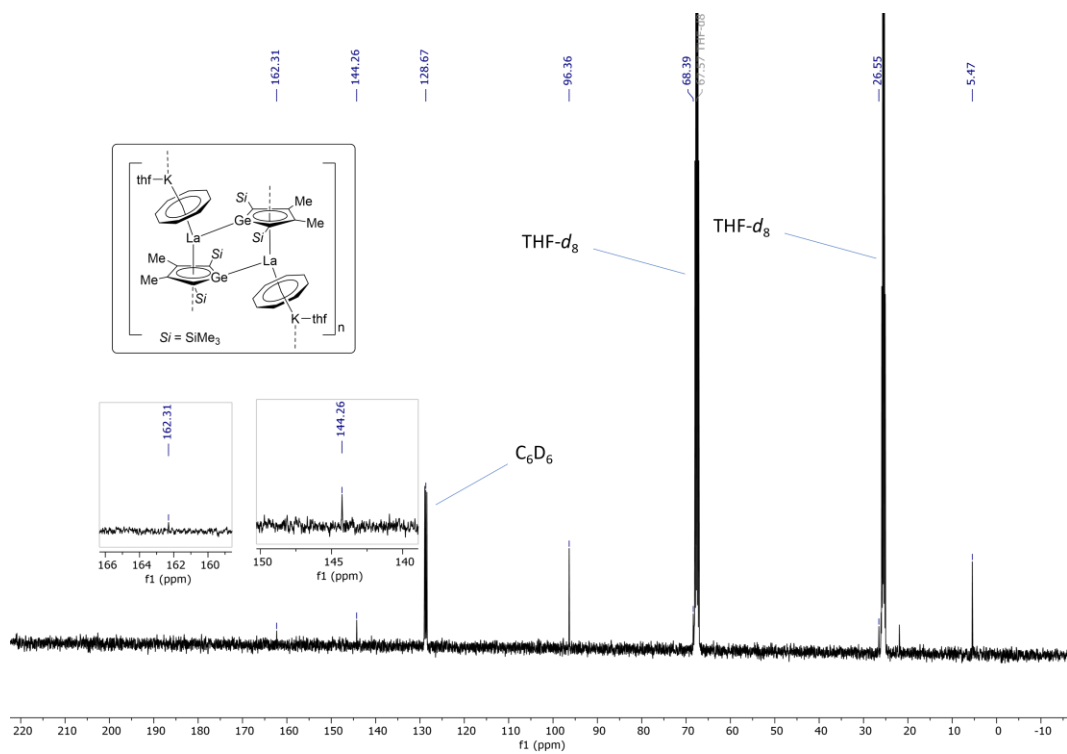
Figure S5. $^{13}C\{^1H\}$ NMR spectrum of compound **2** in THF-d_8/C$_6$D$_6$.
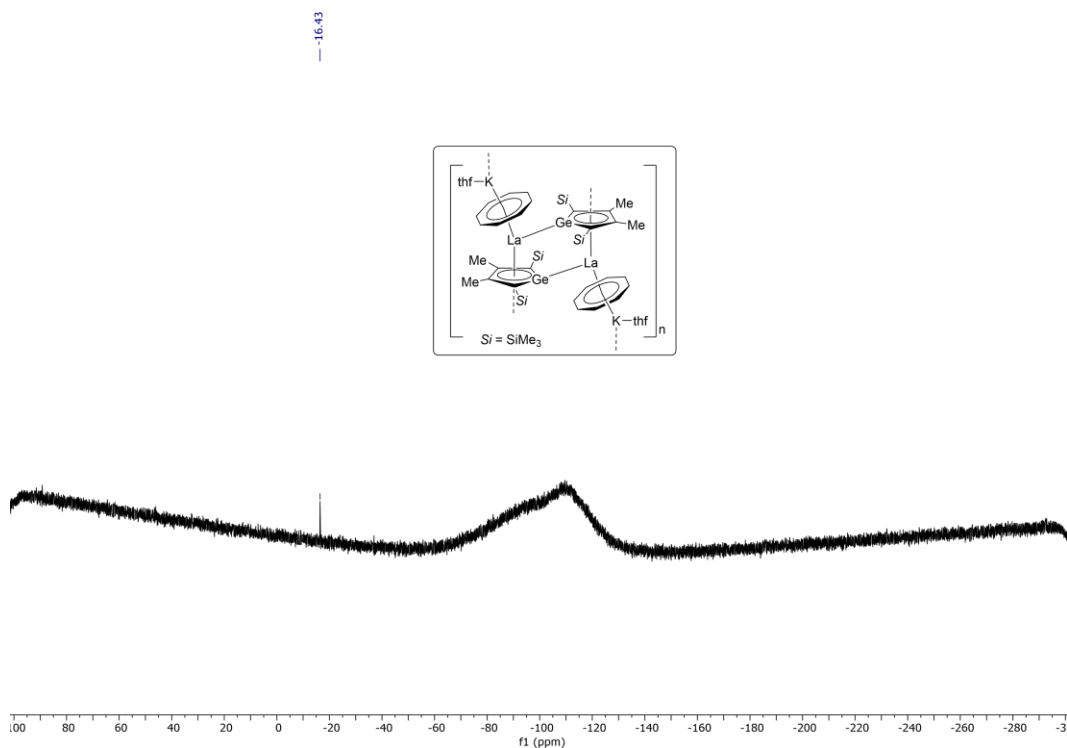

Figure S6. $^{29}Si\{^1H\}$ NMR spectrum of compound **2** in THF-d_8.

7

III. X-ray crystallography

III.1 General methods

Suitable crystals for the X-ray analysis of all compounds were obtained as described above. A suitable crystal was covered in mineral oil (Aldrich) and mounted on a glass fibre. The crystal was transferred directly to the cold stream of a STOE StadiVari (150 K) diffractometer. All structures were solved by using the program SHELXS/T[4,5] and Olex2.[4] The remaining non-hydrogen atoms were located from successive difference Fourier map calculations. The refinements were carried out by using full-matrix least-squares techniques on F^2 by using the program SHELXL.[5,6] The H-atoms were introduced into the geometrically calculated positions (SHELXL procedures) unless otherwise stated and refined riding on the corresponding parent atoms. In each case, the locations of the largest peaks in the final difference Fourier map calculations, as well as the magnitude of the residual electron densities, were of no chemical significance. Specific comments for each data set are given below. Summary of the crystal data, data collection and refinement for compounds are given in Table S1.

Crystallographic data for the structures reported in this paper have been deposited with the Cambridge Crystallographic Data Centre as a supplementary publication no. CCDC 2173290-2173292. Copies of the data can be obtained free of charge on application to CCDC, 12 Union Road, Cambridge CB21EZ, UK (fax: (+(44)1223-336-033; email: deposit@ccdc.cam.ac.uk).

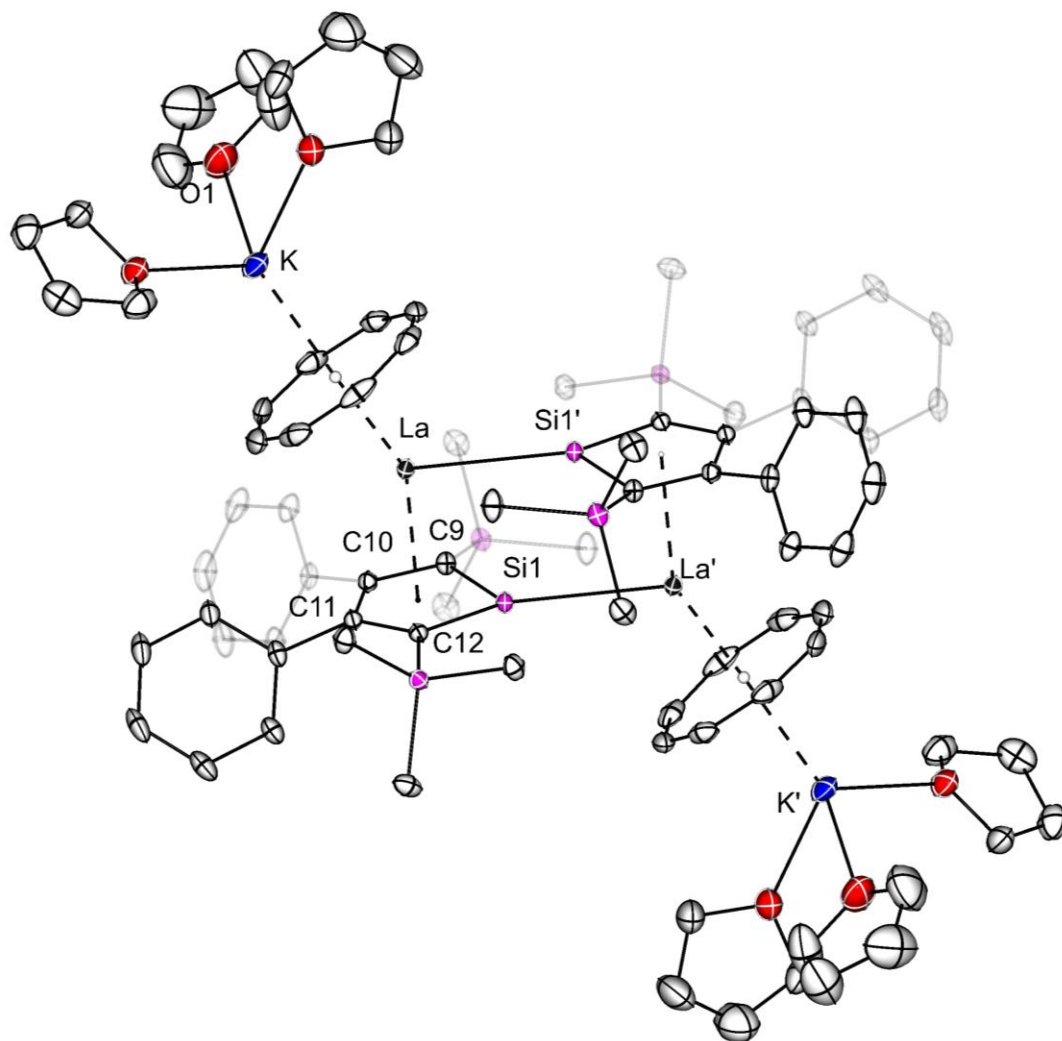The following special comments apply to the models of the structures:

- In the crystal structure of **1**, Fragment DB[7] was used to model one disordered K-bound THF ligand.

- In the crystal structure of **2**, moderate SIMU restraints were applied during the refinement of one disordered, non-coordinating THF moiety.

## III.2 Summary of crystal data

Table S1. Summary of crystal data.

|	1	2	3
Chemical formula	$C_{42}H_{60}KO_3LaSi_2$ ($1.5 \cdot C_4H_8O$)	$C_{48}H_{80}K_2O_2La_2Ge_2Si_4$ ($2 \cdot C_4H_8O$)	$C_{44}H_{56}K_2O_2Ce_2GeSi_2$
CCDC Number	2173290	2173291	2173292
Formula mass	983.33	1446.88	1112.16
Color	red	orange-red	red
Shape	fragment	fragment	block
Radiation type	MoK_α	MoK_α	MoK_α
Wavelength/nm	0.71073	0.71073	0.71073
Crystal system	monoclinic	triclinic	monoclinic
a/Å	15.4366(9)	9.8748(4)	12.9801(7)
b/Å	21.1309(11)	13.1071(7)	23.882(2)
c/Å	15.9239(9)	13.4761(7)	31.570(3)
α/°		108.346(4)	
β/°	107.727(5)	103.835(4)	96.258(6)
γ/°		94.719(4)	
Unit cell volume/Å^3	4950.4(5)	1583.87(14)	9727.9(12)
Temperature/K	150	100	100
Space group	$P2_1/n$	$P\bar{1}$	$C2/c$
Z	4	1	8
Z'	1	0.5	1
Θmax / °	29.509	31.426	28.419
Θmin / °	1.652	2.323	2.313
Absorption coefficient, m/mm	1.060	2.509	2.707
No. of reflections measured	36418	17504	25797
No. of independent reflections	13702	8411	9825
R_{int}	0.0180	0.0427	0.0220
Parameters/Restrains	592/184	378/60	563/132
Largest peak/Deepest hole	1.16/−0.65	2.33/−2.02	1.27/−0.50
Final R_1 values ($I > 2s(I)$)	0.0305	0.0516	0.0299
Final $wR(F^2)$ values ($I > 2s(I)$)	0.0767	0.1378	0.0730
Final R_1 values (all data)	0.0408	0.0623	0.0405
Final $wR(F^2)$ values (all data)	0.0809	0.1439	0.0766
Goodness of fit on F^2	1.026	1.034	1.020

Figure S7. Molecular structure of the complex **1** in the solid state with thermal ellipsoids at 25% level. H atoms and non-coordinating solvent molecules are omitted for clarity. The Me groups of the SiMe$_3$ groups are omitted for clarity. Selected bond distances [Å] and angles [°]: La–Si1' 3.2908(6), La–Si1 3.0888(5), Si1–C9 1.867(2), Si–C12 1.856(2), C9–C10 1.443(3), C10–C11 1.420(3), C11–C12 1.435(3); C9–Si1–C12 90.20(9), Si1–C9–C10 109.21(13), C9–C10–C11 115.3(2), C10–C11–C12 114.8(2), C11–C12–Si1 110.12(14).
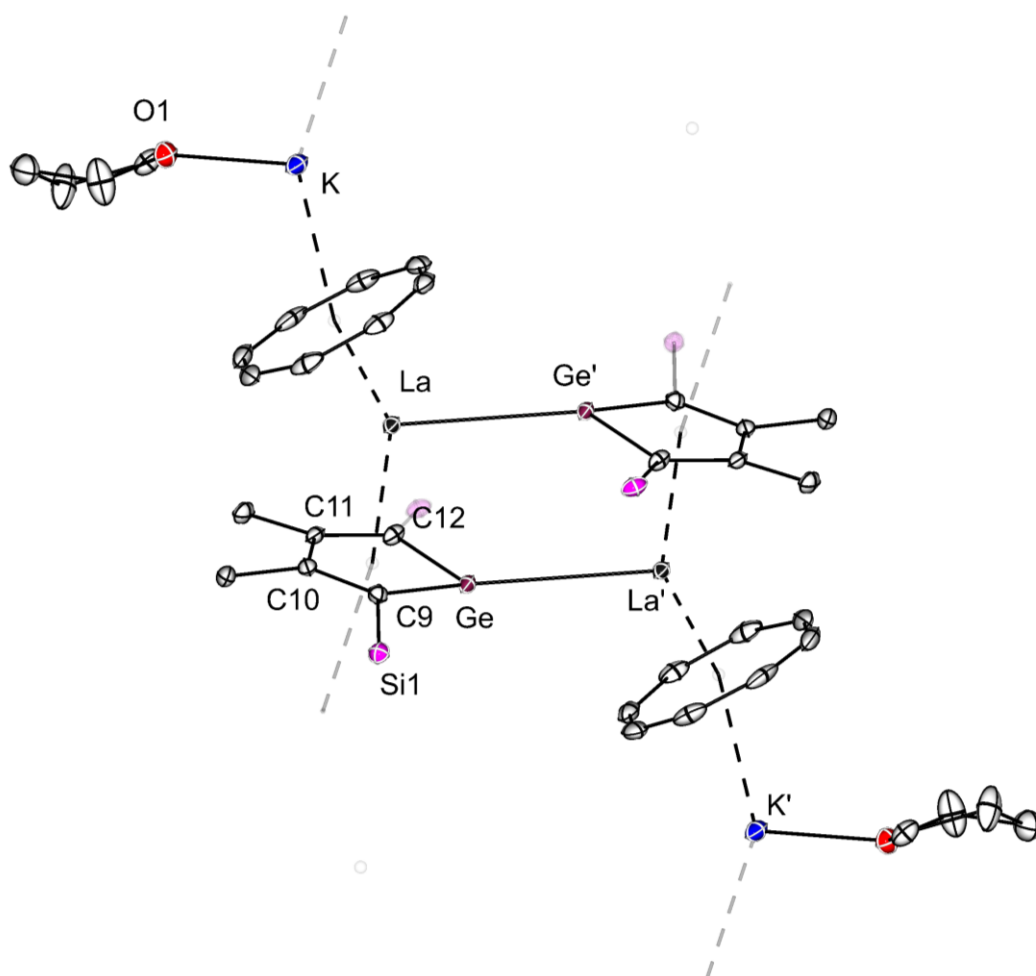
Figure S8. Cut-out of the polymeric structure of **2** in the solid state with thermal ellipsoids at 25% level. H atoms and non-coordinating solvent molecules are omitted for clarity. The Me groups of the SiMe$_3$ groups are omitted for clarity. Selected bond distances [Å] and angles [°]: La–Ge' 3.3048(5), La–Ge 3.1461(4), Ge–C9 1.958(4), Ge–C12 1.945(4), C9–C10 1.426(6), C10–C11 1.426(6), C11–C12 1.435(6); C9–Ge–C12 86.2(2), Ge–C9–C10 110.8(3), C9–C10–C11 116.2(4), C10–C11–C12 115.2(4), C11–C12–Ge 111.4(3).
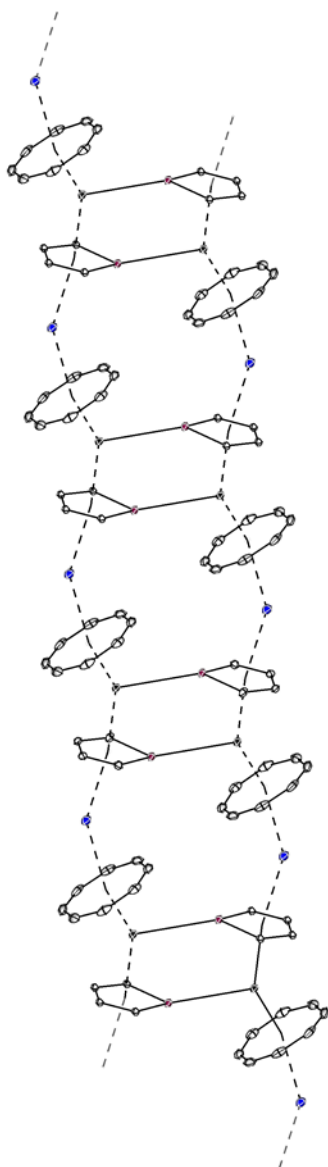
Figure S9. Cut-out of the 1D polymeric chain in compound **2**. All hydrogen atoms, the substituents on the germole ring and the coordinated THF molecules are omitted for clarity.
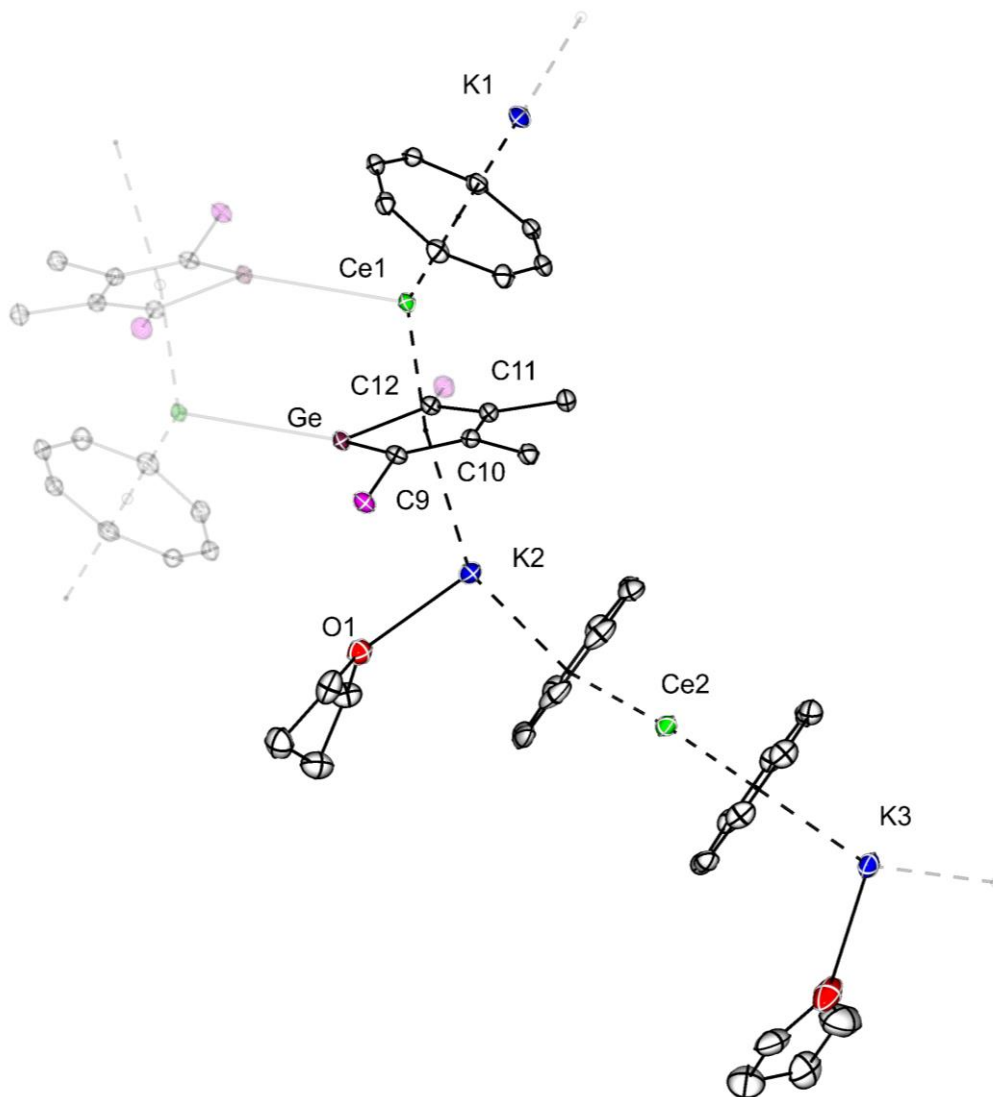
Figure S10. Cut-out of the polymeric structure of **3** in the solid state with thermal ellipsoids at 25% level. H atoms and non-coordinating solvent molecules are omitted for clarity. The Me groups of the SiMe$_3$ groups are omitted for clarity. Selected bond distances [Å] and angles [°]: Ce1–Ge' 3.2158(4), Ce–Ge 3.1088(4), Ge–C9 1.956(3), Ge–C12 1.952(3), C9–C10 1.436(4), C10–C11 1.416(5), C11–C12 1.434(4); C9–Ge–C12 86.46(13), Ge–C9–C10 110.5(2), C9–C10–C11 116.0(3), C10–C11–C12 116.1(3), C11–C12–Ge 110.7(2).

IV. Reference

1   Z. Dong, C. R. W. Reinhold, M. Schmidtmann and T. Müller, *Organometallics*, 2018, **37**, 4736-4743.

2   L. Münzfeld, C. Schoo, S. Bestgen, E. Moreno-Pineda, R. Köppe, M. Ruben and P. W. Roesky, *Nat. Commun.*, 2019, **10**, 3135.

3   K. Mashima, Y. Nakayama, A. Nakamura, N. Kanehisa, Y. Kai and H. Takaya, *J. Organomet. Chem.*, 1994, **473**, 85-91.

4   G. Sheldrick, *Acta Crystallogr A*, 2008, **64**, 112-122.

5   G. Sheldrick, *Acta Crystallogr*. C, 2015, **71**, 3-8.

6   O. V. Dolomanov, L. J. Bourhis, R. J. Gildea, J. A. K. Howard and H. Puschmann, *J. Appl. Crystallogr.*, 2009, **42**, 339-341.

7   D. Kratzert, I. Krossing, *J. Appl. Cryst.* 2018, **51**, 928-934.